

## Research Article

# Nonenzymatic Glucose Sensor Based on Porous $\text{Co}_3\text{O}_4$ Nanoneedles

Jianchun Sun <sup>1</sup>, Hongjing Zhao <sup>2</sup>, and Zhongchang Wang <sup>1,3</sup>

<sup>1</sup>College of Metallurgy and Materials Engineering, Chongqing University of Science and Technology, Chongqing 401331, China

<sup>2</sup>Chongqing Ecological Environment Monitoring Center, Chongqing 400030, China

<sup>3</sup>International Iberian Nanotechnology Laboratory, Braga 4715-330, Portugal

Correspondence should be addressed to Jianchun Sun; [jianchunsun@cqust.edu.cn](mailto:jianchunsun@cqust.edu.cn) and Hongjing Zhao; [zjzhj@163.com](mailto:zjzhj@163.com)

Received 20 July 2022; Accepted 14 September 2022; Published 8 October 2022

Academic Editor: Tianming Li

Copyright © 2022 Jianchun Sun et al. This is an open access article distributed under the Creative Commons Attribution License, which permits unrestricted use, distribution, and reproduction in any medium, provided the original work is properly cited.

Herein, porous  $\text{Co}_3\text{O}_4$  nanoneedle arrays were synthesized on nickel (Ni) foam ( $\text{Co}_3\text{O}_4$  NNs/NF) by one-step hydrothermal method. Some electrochemical methods were used to investigate its nonenzymatic glucose sensing performance in alkaline solution. The results show that the sensitivity of  $\text{Co}_3\text{O}_4$  NNs/NF electrode to glucose is  $4570 \mu\text{A mM}^{-1} \text{cm}^{-2}$ . The linear range is  $1 \mu\text{M}$ – $0.337 \text{mM}$ , and the detection limit is  $0.91 \mu\text{M}$  ( $S/N = 3$ ). It also displays good selectivity and repeatability for glucose. The good electrochemical sensing performance of  $\text{Co}_3\text{O}_4$  NNs/NF based sensor for glucose can be attributed to interconnected porous structure and large specific surface area of  $\text{Co}_3\text{O}_4$ .

## 1. Introduction

Rapid and accurate detection of blood glucose concentration is very important for the diagnosis and treatment of diabetes. Although graphene oxide based glucose sensor dominates the market, it has some defects, such as high cost, limited stability, and complex enzyme immobilization process [1, 2]. In recent years, nonenzymatic glucose sensors have attracted the attention of a large number of researchers because of their advantages such as low cost, good stability, fast response, and simple fabrication [3].

Electrocatalytic active materials modified on the electrode surface have a great impact on the performance of nonenzymatic glucose sensor [4]. So far, a series of nanostructured materials based on precious metals and their alloys (such as Pt, Ag, Pd, Au, Pt-Pd, and Pt-Au) have excellent electrochemical catalytic oxidation activity, which has been proved to be used for the electrocatalytic oxidation of glucose [5–8]. However, due to the scarcity and high cost of these precious metals, the surface of precious metal based materials is usually easily polluted by adsorbed intermediates and chloride ions, which greatly affects the stability and sensitivity of the sensor [9, 10]. In view of this, researchers try to

develop electrode materials with high performance and low cost for nonenzymatic glucose sensing. In particular, transition metal oxides have the advantages of low price and high conductivity. They are regarded as the ideal electrode active materials for nonenzymatic glucose sensing [11, 12]. Among them,  $\text{Co}_3\text{O}_4$  is an ionic semiconductor with both polar positive electrodes (two  $\text{Co}^{2+}$ , two  $\text{Co}^{3+}$ , and four  $\text{O}^{2-}$ ) and polar negative electrodes (two  $\text{Co}^{3+}$  and four  $\text{O}^{2-}$ ). It has excellent electrochemical performance and has been widely used in photocatalysis, supercapacitors, lithium-ion batteries, electrochemical sensors, and other fields [13]. Therefore,  $\text{Co}_3\text{O}_4$ , which has good lasting stability and electrocatalytic activity in alkaline medium, is also one of the most promising materials for electrocatalytic oxidation of glucose.

As we all know, different morphologies and microstructures of materials would produce substantial differences in their surface area, particle size, pore structure, mass transfer, and electron transfer efficiency, which will affect their electrochemical sensing performance [14]. Therefore, construction of  $\text{Co}_3\text{O}_4$  with excellent microstructure can effectively enhance the electrocatalytic performance of glucose. If the  $\text{Co}_3\text{O}_4$  catalytic material is directly grown on the conductive substrate in the form of well-arranged nanoarrays, the

performance of the catalytic material can be effectively improved. In this work, one-step hydrothermal method was used to prepare porous  $\text{Co}_3\text{O}_4$  nanoneedle arrays ( $\text{Co}_3\text{O}_4$  NNs/NF) in situ on Ni foam. With the help of the three electrode system, the electrochemical performance of the self-supporting electrode in situ was tested. The results show that  $\text{Co}_3\text{O}_4$  NNs/NF exhibits higher sensitivity, lower detection limit, good repeatability, and good excellent selectivity for common interfering substances.

## 2. Materials and Methods

**2.1. Preparation of  $\text{Co}_3\text{O}_4$  NNs/NF. Pretreatment of Ni Foam:** firstly, an area of  $2 \times 4 \text{ cm}^2$  Ni foam was sonicated in the HCl solution (2 M), anhydrous ethanol, deionized water for 15 min, respectively, and then, the cleaned Ni foam was dried at  $60^\circ\text{C}$ .

**Preparation of  $\text{Co}_3\text{O}_4$  NNs/NF:** 5 mmol of  $\text{Co}(\text{N}-\text{O}_3)_2 \cdot 6\text{H}_2\text{O}$  and 4.5 mmol of urea were solved into 30 mL of deionized water. After stirring, 2 mmol of cetyltrimethyl ammonium bromide (CTAB) was added into the above solution and stirred at  $45^\circ\text{C}$  for 30 min. Subsequently, the uniform solution was transferred into the Teflon-sealed autoclave, and the cleaned Ni foam was inserted into the inner container by tweezers, and the Ni foam was completely immersed in the solution. Then the autoclave was sealed and placed in the electric hot air drying oven, and then heated continuously for 6 h at  $120^\circ\text{C}$ . When the autoclave naturally cooled to room temperature, the autoclave was opened, and the Ni foam with precursor was collected by tweezers and washed repeatedly with ethanol and distilled water. Then, the Ni foam was put it into a drying oven with a temperature set at  $60^\circ\text{C}$  for 8 h. Finally, the Ni foam with precursor was placed in a clean crucible and then baked in a muffle furnace. The heating rate was set at  $1^\circ\text{C}/\text{min}$ , heated to  $350^\circ\text{C}$ , and continuously calcined 2 h.

**2.2. Electrochemical Performance Test.** In current work, we prepared the sensing material on the surface of Ni foam. The thickness of sensing film is about 0.1 mm. During the electrochemical test, the RST-5000F electrochemical workstation was used for electrochemical test. The freshly prepared NaOH (0.1 M) solution was served as the electrolyte. Cyclic voltammetry and chronoamperometry were performed at room temperature.  $\text{Co}_3\text{O}_4$  NNs/NF ( $1 \times 2 \text{ cm}^2$ ), Ag/AgCl electrode, and Pt sheet electrode were used as working electrode, reference electrode, and counter electrode, respectively. The humidity in current work is 30 RH%.

## 3. Results and Discussion

The prepared sample was obtained from the Ni foam by ultrasonic wave, and the composition of the sample was studied by XRD. The XRD pattern of  $\text{Co}_3\text{O}_4$  arrays on Ni foam is shown in Figure 1. The obvious diffraction peaks at  $19.0^\circ$ ,  $31.2^\circ$ ,  $36.8^\circ$ ,  $38.5^\circ$ ,  $44.8^\circ$ ,  $55.6^\circ$ ,  $59.3^\circ$ , and  $65.2^\circ$  are corresponding to (111), (220), (311), (222), (400), (422), (511), and (440) planes of cubic phase  $\text{Co}_3\text{O}_4$  (JCPDS No. 42-1467). Moreover, no other impurity peaks are found in

the pattern, which indicates that the as-prepared  $\text{Co}_3\text{O}_4$  sample has good crystallinity and high purity.

Figure 2(a) displays the SEM image of  $\text{Co}_3\text{O}_4$  NNs/NF electrode at low magnification. It can be seen that  $\text{Co}_3\text{O}_4$  nanoneedles are evenly covered on the conductive substrate, and there is a gap between the nanoneedles, which is conducive to the diffusion of electrolyte and the escape of bubbles on the electrode surface, so as to improve the catalytic activity. From the high magnified SEM image in Figure 2(b), it can be found that the diameter of  $\text{Co}_3\text{O}_4$  nanoneedles is about 80-100 nm, and its surface is rough and uneven, which may be porous structure. Subsequently,  $\text{Co}_3\text{O}_4$  nanoneedles were dispersed in ethanol by ultrasonic method and characterized by TEM technique. Figure 2(c) shows that the nanoneedles with a diameter of about 100 nm are actually composed of interconnected single nanoparticles, which is consistent with the SEM observation. Such highly porous nanoneedle structure is helpful for the rapid diffusion of electrolyte ions in the electrode and accelerates electron transfer, so that the as-prepared  $\text{Co}_3\text{O}_4$  electrode may have good electrochemical performance. Additionally, the HR-TEM image of  $\text{Co}_3\text{O}_4$  nanoneedles (Figure 2(d)) shows that there are two groups of clear lattice fringes. It is found that their fringe spacing is 0.242 nm and 0.465 nm, respectively, which exactly corresponds to the (311) and (111) crystal planes of  $\text{Co}_3\text{O}_4$  standard diffraction spectrum (JCPDS 42-1467). These results further confirm the successful synthesis of porous  $\text{Co}_3\text{O}_4$  nanoneedles on Ni foam.

Using a typical three electrode system, the electrocatalytic activity of  $\text{Co}_3\text{O}_4$  NNs/NF for glucose oxidation was investigated by cyclic voltammetry. Figure 3(a) shows the CV curve of  $\text{Co}_3\text{O}_4$  NNs/NF in the absence and presence of 0.6 mM glucose at a scanning speed of  $10 \text{ mV s}^{-1}$ . Obviously, the oxidation peak current of  $\text{Co}_3\text{O}_4$  NNs/NF at 0.55 V increases significantly after the addition of 0.6 mM glucose. In addition, Figure 3(b) shows the CV curve of  $\text{Co}_3\text{O}_4$  NNs/NF when the glucose concentration in 0.1 M, the NaOH solution is 0 mM, 0.2 mM, 0.4 mM, and 0.6 mM, respectively (the scanning speed is set to  $10 \text{ mV s}^{-1}$ ). With the increase of glucose concentration, the peak current also increases. The above results show that the prepared  $\text{Co}_3\text{O}_4$  NNs/NF has good electrocatalytic activity for glucose oxidation, and the specific process can be described as [15, 16]

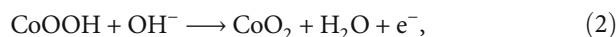
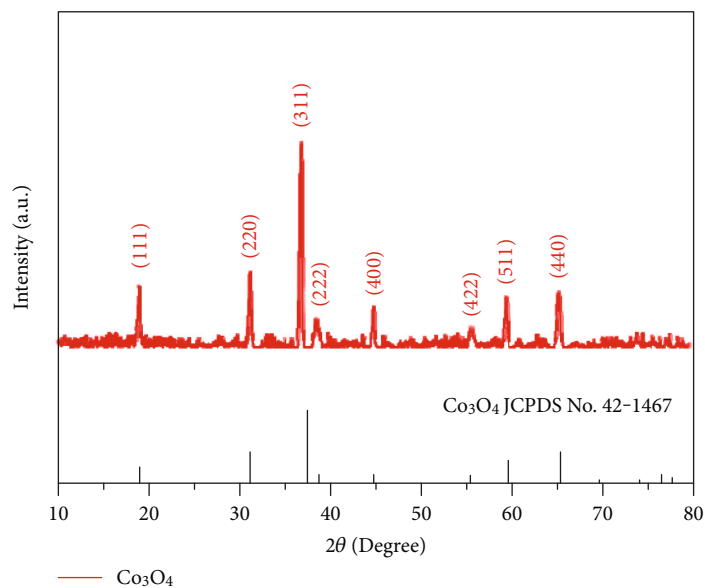
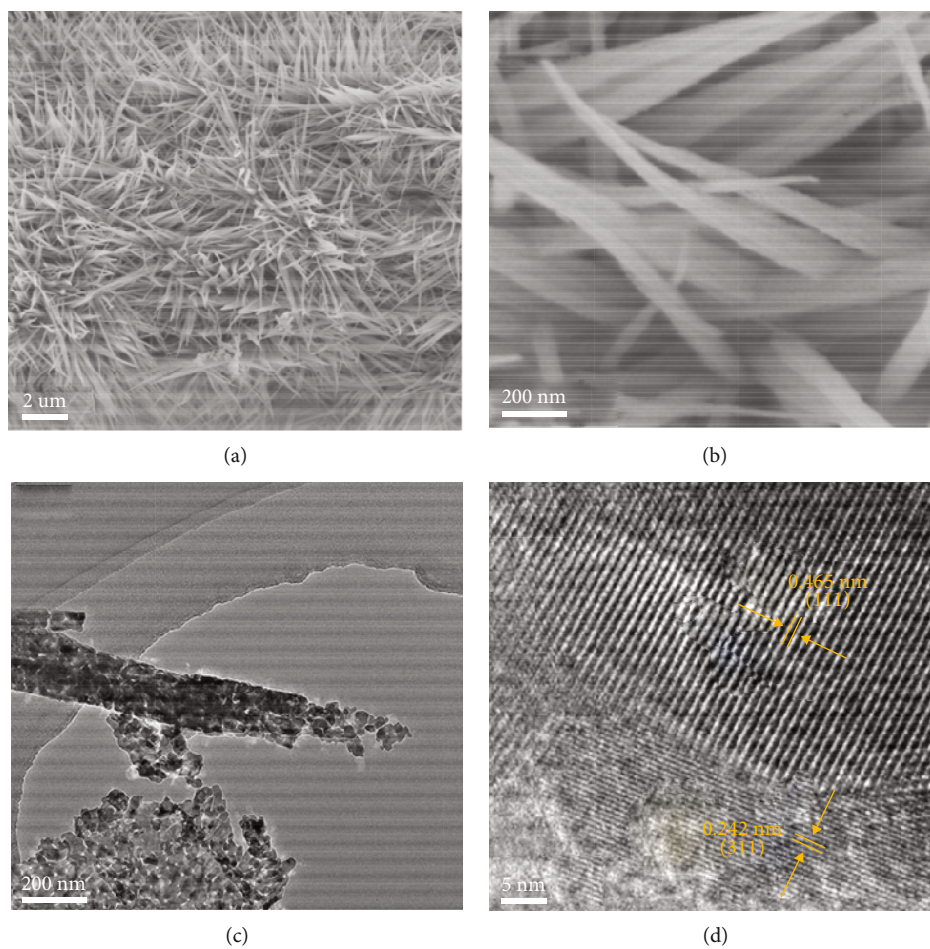


Figure 3(c) shows the CV curve of  $\text{Co}_3\text{O}_4$  NNs/NF electrode at different scanning rates ( $5-50 \text{ mV s}^{-1}$ ) in the presence of 0.8 mM glucose in 0.1 M NaOH. The peak current of anode and cathode increases with the increase of scanning rate. It can be seen from Figure 3(d) that the peak current of anode and cathode has a good linear relationship with the square root of scanning rate, and the correlation coefficients are 0.99381 and 0.99893, respectively, indicating that the

FIGURE 1: XRD pattern of  $\text{Co}_3\text{O}_4$  NNs.FIGURE 2: SEM images of  $\text{Co}_3\text{O}_4$  NNs/NF at (a) low magnification and (b) high magnification. (c) TEM and (d) HR-TEM images of  $\text{Co}_3\text{O}_4$  NNs.

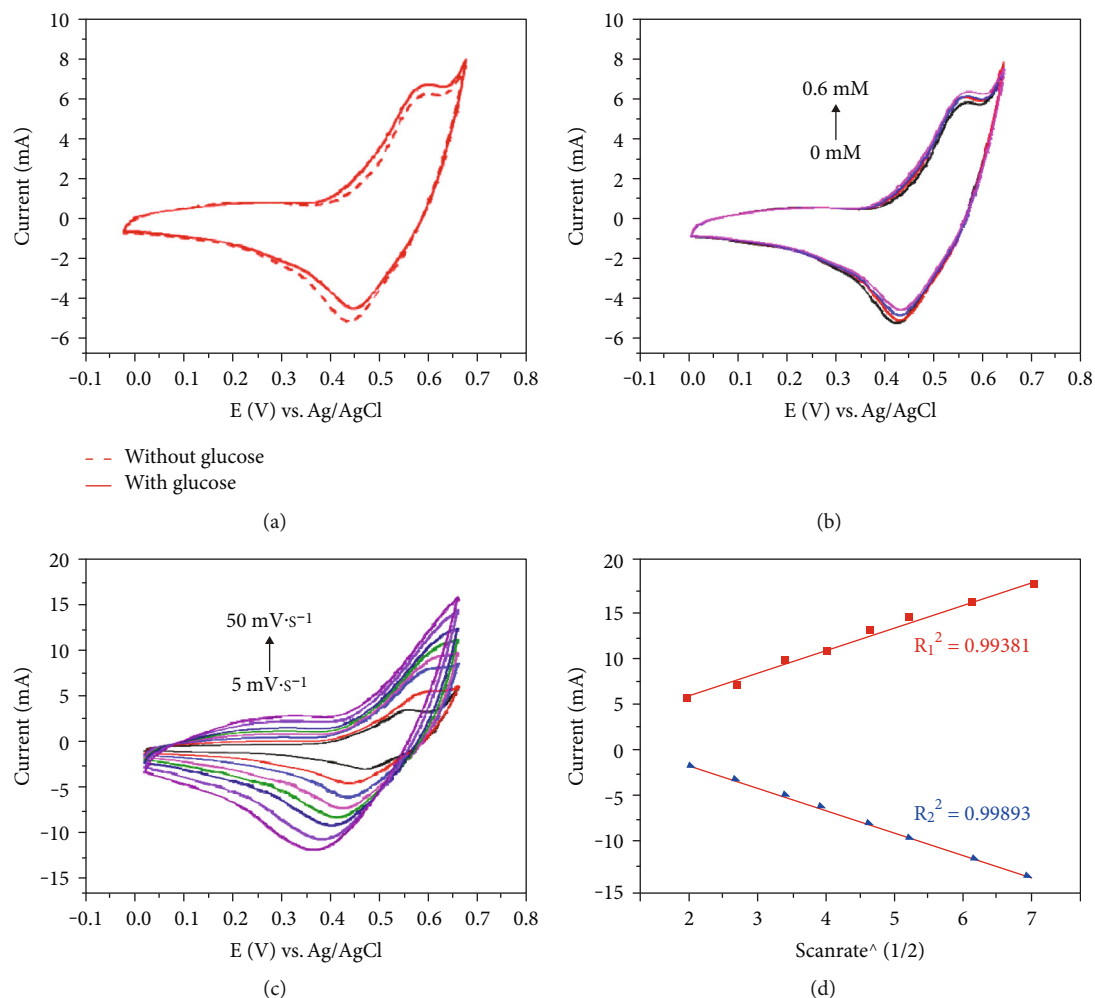


FIGURE 3: CV curves of  $\text{Co}_3\text{O}_4$  NNs/NF (a) with and without glucose, (b) at different glucose concentration, (c) at different scan rates, and (d) the corresponding linear relationship between the anodic/cathodic peak currents and the square root of scanning rate ( $v^{1/2}$ ).

oxidation process of glucose on  $\text{Co}_3\text{O}_4$  NNs/NF is a diffusion controlled process [17].

Chronoamperometry technology was carried out to evaluate the sensitivity, detection limit, and selectivity of the electrode to glucose. Under the condition of working voltage of 0.55 V,  $\text{Co}_3\text{O}_4$  NNs/NF electrode was tested, and glucose solutions with different concentrations were gradually added to 0.1 M NaOH solution. As shown in Figure 4(a), when glucose of different concentrations is added to the alkaline solution in the state of uniform stirring at an interval of 50 s, it can be seen that the current response is relatively rapid and the curve is similar to a ladder. In addition, Figure 4(b) shows the corresponding relationship between glucose concentration and current in this process. In the range of 1  $\mu\text{M}$ –0.338 mM, the concentration and current have good linear correlation. Its linear regression equation can be expressed as  $I$  (mA) = 9.14C (mM) + 0.097 ( $R^2 = 0.99017$ ), and the sensitivity is 4570  $\mu\text{A mM}^{-1} \text{cm}^{-2}$ . The detection limit (LOD) for glucose is about 0.91  $\mu\text{M}$  ( $S/N = 3$ ), and its response time is about 8 s (Figure 4(c)).

Since there are other interfering substances in real human serum, which may also be oxidized, it is necessary to test the anti-interference ability of  $\text{Co}_3\text{O}_4$  NNs/NF electrode. Here, the typical disruptors were selected, such as uric acid (UA), ascorbic acid (AA), fructose, and sucrose for electrochemical detection by chronoamperometry. Because the concentration of blood glucose in normal human serum is 30–50 times that of these interfering substances [18], 1.0 mM glucose and 0.1 mM interfering substances were added for testing. It can be seen from Figure 4(d) that the current density increases significantly after adding 1.0 mM glucose, but there is no significant change in current density after adding other interferents. Therefore,  $\text{Co}_3\text{O}_4$  NNs/NF has good selectivity for glucose detection.

Repeatability and stability are also important indicators to evaluate the operability and durability of the prepared nonenzymatic glucose sensor electrode. Five  $\text{Co}_3\text{O}_4$  NNs/NF electrodes were prepared by the same method, and the prepared electrodes were tested by cyclic voltammetry under the same conditions. Their respective peak oxidation

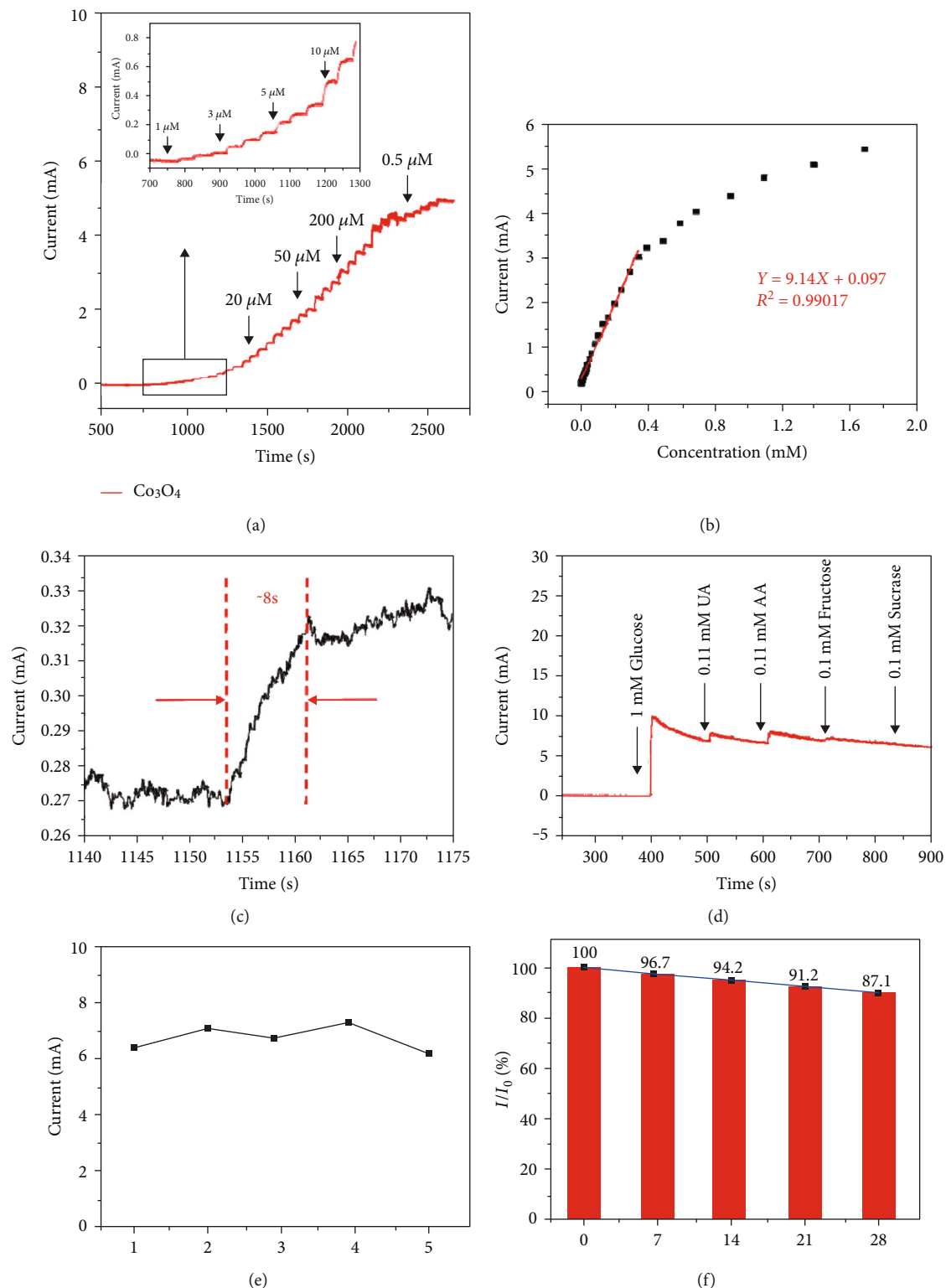


FIGURE 4: (a) The amperometric response of  $\text{Co}_3\text{O}_4$  NNs/NF when glucose was continuously injected into 0.1 M NaOH solution at 0.55 V; the inset showed the enlarged response curve from the black rectangle. (b) Calibration curve between current response and glucose concentration. (c) The response time of  $\text{Co}_3\text{O}_4$  NNs/NF. (d) The amperometric response of  $\text{Co}_3\text{O}_4$  NNs/NF to the sequential addition of 1 mM glucose and 0.1 mM different interferences (UA, AA, fructose, and sucrose); Potential: 0.55 V. (e) The peak oxidation currents of  $\text{Co}_3\text{O}_4$  NNs/NF fabricated in five batches via the same method. (f) Storage stability of  $\text{Co}_3\text{O}_4$  NNs/NF tested by CV.

currents were recorded. As shown in Figure 4(e), its relative standard deviation (RSD) is 7.1%, which has good repeatability. In order to study the stability of the electrode, the  $\text{Co}_3\text{O}_4$  NNs/NF electrode was placed at room temperature for 28 days, and the cyclic voltammetry test was carried out every 7 days. The oxidation current of the electrode maintains 87.1% of its initial value on the 28th day (Figure 4(f)), indicating good stability of the  $\text{Co}_3\text{O}_4$  NNs/NF electrode. It can be attributed to that the active material is evenly and firmly grown on the conductive Ni foam, leading to the stable structure. It is not easy to collapse or agglomeration, so it has good repeatability and stability.

#### 4. Conclusions

In this work, a simple one-step hydrothermal synthesis method of  $\text{Co}_3\text{O}_4$  NNs/NF is proposed for the detection of nonenzymatic glucose. The sensor based on  $\text{Co}_3\text{O}_4$  NNs/NF has good sensitivity to glucose ( $4570 \mu\text{A mM}^{-1} \text{cm}^{-2}$ ) and low detection limit ( $0.91 \mu\text{M}$ ). The linear detection range is  $1 \mu\text{M}$ – $0.337 \text{ mM}$ . Moreover, it has good selectivity and stability for glucose. At the 28th day, its oxidation response current still maintains 87.1% of its initial value. The good electrochemical sensing performance of  $\text{Co}_3\text{O}_4$  NNs/NF based sensor for glucose can be attributed to the following factors: on the one hand, the firm and evenly arranged  $\text{Co}_3\text{O}_4$  nanoneedles grown directly on the conductive substrate can prevent the blockage of active sites caused by additional adhesives, so as to ensure efficient electron transfer. On the other hand, the ordered and interconnected porous structure and large specific surface area can not only provide more active sites for electrochemical reactions but also enhance the contact between active substances.

#### Data Availability

The data used to support the findings of this study are available from the corresponding author upon request.

#### Conflicts of Interest

The authors declare that they have no conflicts of interest.

#### Acknowledgments

This work was supported by the Natural Science Foundation of Chongqing (Grant No. 2022NSCQ-MSX4128).

#### References

- [1] R. Wilson and A. P. F. Turner, "Glucose oxidase: an ideal enzyme," *Biosensors and Bioelectronics*, vol. 7, no. 3, pp. 165–185, 1992.
- [2] A. Meng, X. Yuan, Z. Li, K. Zhao, L. Sheng, and Q. Li, "Direct growth of 3D porous (Ni-Co) $_3\text{S}_4$  nanosheets arrays on rGO-PEDOT hybrid film for high performance non-enzymatic glucose sensing," *Sensors and Actuators B: Chemical*, vol. 291, no. 15, pp. 9–16, 2019.
- [3] Q. Dong, H. Ryu, and Y. Lei, "Metal oxide based non-enzymatic electrochemical sensors for glucose detection," *Electrochimica Acta*, vol. 370, no. 20, article 137744, 2021.
- [4] W. B. Kim, S. H. Lee, M. Cho, and Y. Lee, "Facile and cost-effective CuS dendrite electrode for non-enzymatic glucose sensor," *Sensors and Actuators B: Chemical*, vol. 249, pp. 161–167, 2017.
- [5] R. Wang, X. Liu, Y. Zhao et al., "Novel electrochemical non-enzymatic glucose sensor based on 3D Au@Pt core-shell nanoparticles decorated graphene oxide/multi-walled carbon nanotubes composite," *Microchemical Journal*, vol. 174, article 107061, 2022.
- [6] Y. Fan, X. Tan, X. Ou, S. Chen, and S. Wei, "An ultrasensitive electrochemiluminescence biosensor for the detection of concanavalin A based on Au nanoparticles-thiosemicarbazide functionalized PtNi nanocubes as signal enhancer," *Biosensors and Bioelectronics*, vol. 87, no. 15, pp. 802–806, 2017.
- [7] M. Usman, L. Pan, A. Farid et al., "Ultra-fast and highly sensitive enzyme-free glucose sensor based on 3D vertically aligned silver nanoplates on nickel foam-graphene substrate," *Journal of Electroanalytical Chemistry*, vol. 848, no. 1, article 113342, 2019.
- [8] M. Shen, W. Li, L. Chen, Y. Chen, S. Ren, and D. Han, "NiCo-LDH nanoflake arrays-supported Au nanoparticles on copper foam as a highly sensitive electrochemical non-enzymatic glucose sensor," *Analytica Chimica Acta*, vol. 1177, no. 8, article 338787, 2021.
- [9] D. W. Hwang, S. Lee, M. Seo, and T. D. Chung, "Recent advances in electrochemical non-enzymatic glucose sensors - a review," *Analytica Chimica Acta*, vol. 1033, no. 29, pp. 1–34, 2018.
- [10] D. Ge, Y. Yang, X. Ni et al., "Self-template formation of porous  $\text{Co}_3\text{O}_4$  hollow nanoprisms for non-enzymatic glucose sensing in human serum," *RSC Advances*, vol. 10, no. 63, pp. 38369–38377, 2020.
- [11] X. Niu, Y. Li, J. Tang, Y. Hu, H. Zhao, and M. Lan, "Electrochemical sensing interfaces with tunable porosity for nonenzymatic glucose detection: A Cu foam case," *Biosensors and Bioelectronics*, vol. 51, no. 15, pp. 22–28, 2014.
- [12] L. Jiang, S. Gu, Y. Ding, F. Jiang, and Z. Zhang, "Facile and novel electrochemical preparation of a graphene-transition metal oxide nanocomposite for ultrasensitive electrochemical sensing of acetaminophen and phenacetin," *Nanoscale*, vol. 6, no. 1, pp. 207–214, 2014.
- [13] M. Yang, J. M. Jeong, K. G. Lee, D. H. Kim, S. J. Lee, and B. G. Choi, "Hierarchical porous microspheres of the  $\text{Co}_3\text{O}_4$ @graphene with enhanced electrocatalytic performance for electrochemical biosensors," *Biosensors and Bioelectronics*, vol. 89, Part 1, pp. 612–619, 2017.
- [14] W. Li, D. Liu, X. Feng, Z. Zhang, X. Jin, and Y. Zhang, "High-performance ultrathin  $\text{Co}_3\text{O}_4$  nanosheet supported PdO/CeO $_2$  catalysts for methane combustion," *Advanced Energy Materials*, vol. 9, no. 18, article 1803583, 2019.
- [15] A. T. E. Vilian, B. Dinesh, M. Rethinasabapathy et al., "Hexagonal  $\text{Co}_3\text{O}_4$  anchored reduced graphene oxide sheets for high-performance supercapacitors and non-enzymatic glucose sensing," *Journal of Materials Chemistry A*, vol. 6, no. 29, pp. 14367–14379, 2018.
- [16] M. Zheng, L. Li, P. Gu, Z. Lin, H. Xue, and H. Pang, "A glassy carbon electrode modified with ordered nanoporous  $\text{Co}_3\text{O}_4$  for non-enzymatic sensing of glucose," *Microchimica Acta*, vol. 184, no. 3, pp. 943–949, 2017.

- [17] D. Yin, X. Bo, J. Liu, and L. Guo, "A novel enzyme-free glucose and  $H_2O_2$  sensor based on 3D graphene aerogels decorated with  $Ni_3N$  nanoparticles," *Analytica Chimica Acta*, vol. 1038, pp. 11–20, 2018.
- [18] I. U. Hassan, H. Salim, G. A. Naikoo et al., "A review on recent advances in hierarchically porous metal and metal oxide nanostructures as electrode materials for supercapacitors and non-enzymatic glucose sensors," *Journal of Saudi Chemical Society*, vol. 25, no. 5, article 101228, 2021.